

# PRELIMINARY CHEMOMETRIC STUDY OF BONE DIAGENESIS IN EARLY TRIASSIC CYNODONTS FROM MENDOZA, ARGENTINA



ELENA PREVITERA<sup>1</sup>, JOSÉ A. D'ANGELO<sup>1,2</sup> AND ADRIANA C. MANCUSO<sup>1</sup>

<sup>1</sup>Instituto Argentino de Nivología, Glaciología y Ciencias Ambientales (IANIGLA), CCT-CONICET-Mendoza, Avda. Ruiz Leal s/n Parque Gral. San Martín, C.C. 330, 5500 Mendoza, Argentina. [eprevitera@mendoza-conicet.gov.ar](mailto:eprevitera@mendoza-conicet.gov.ar); [amancu@mendoza-conicet.gov.ar](mailto:amancu@mendoza-conicet.gov.ar)

<sup>2</sup>Área de Química, Instituto de Ciencias Básicas, Universidad Nacional de Cuyo, Centro Universitario, M5502JMA Mendoza, Argentina. [joseadangelo@yahoo.com](mailto:joseadangelo@yahoo.com)

**Abstract.** The non-mammalian therapsids dominated the terrestrial ecosystems during the Late Paleozoic–Early Mesozoic. The cynodonts have been studied from a taxonomic, osteologic and morphological perspective. However, taphonomy using chemometrics has been barely explored. This report includes a rib and an appendicular bone of cynodonts from the Puesto Viejo Group (Mendoza, Argentina). These fossils are studied for the first time using SEM-EDX. Semi-quantitative data derived from SEM-EDX spectra is evaluated by principal component analysis to gain new insights regarding the different diagenetic pathways of bone microstructure. The multivariate model supports the distinction of different sampled areas (bone, transition zone and rock matrix), in terms of chemical parameters. Differentiation is based mainly on varying contents of Ca, P, F, Si, Al, K, O, Mn and Fe. Variable concentrations of Fe and Mn could be related to different facies (floodplain and crevasse splay). These results along with thin section petrographical analysis confirm –in one of the cases– the substitution of hydroxyapatite by fluorapatite in the bone microstructure. Fossil-diagenetic processes observed herein include substitution, fracturing, brittle deformation and different permineralization events. Permineralization stages during burial history include infilling of vascular canals, trabeculae and fractures with hematite, manganite and calcite. The presence of calcite and iron enrichment indicates local reducing conditions below water-table during precipitation. This chemometric approach to the study of Triassic cynodont remains proved useful for assessing the chemical changes in bone microstructure.

**Keywords.** Puesto Viejo Group. Fossil-diagenesis. Mesozoic. Non-mammaliaform therapsids. Chemometrics.

**Resumen.** ESTUDIO QUIMIOMÉTRICO PRELIMINAR DE DIAGÉNESIS ÓSEA EN CINODONTES DEL TRIÁSICO TEMPRANO DE MENDOZA, ARGENTINA. Los terápsidos no-mamaliformes dominaron los ecosistemas terrestres durante el Paleozoico Tardío–Mesozoico Temprano. Los cinodontes han sido estudiados desde una perspectiva taxonómica, osteológica y morfológica. Sin embargo, análisis tafonómicos usando quimiometría son escasos. Esta contribución incluye una costilla y un hueso apendicular de cinodontes del Grupo Puesto Viejo (Mendoza, Argentina). Estos fósiles se analizaron por primera vez usando SEM-EDX. Los datos semi-cuantitativos derivados de SEM-EDX se evaluaron mediante análisis de componentes principales para obtener nuevos conocimientos sobre las diferentes vías diagenéticas de la microestructura ósea. El modelo multivariado apoya la distinción de las diferentes áreas de la muestra (hueso, zona de transición y matriz rocosa), en términos de parámetros químicos. La diferenciación se basa principalmente en diferentes contenidos de Ca, P, F, Si, Al, K, O, Mn y Fe. Concentraciones variables de Fe y Mn pueden asociarse a las diferentes facies (planicie de inundación y depósitos de desbordamiento). Estos resultados, junto con los análisis petrográficos de secciones delgadas confirman en uno de los casos la sustitución de la hidroxiatapita por fluorapatita en la microestructura ósea. Los procesos fósildiagenéticos observados incluyen sustitución, fracturación, deformación frágil y diferentes eventos de permineralización. Las etapas de permineralización incluyen rellenos de hematita, manganita y calcita, en canales vasculares, trabéculas y fracturas, durante el enterramiento. La presencia de calcita y de hierro indica condiciones reductoras locales bajo el nivel freático durante la precipitación. Este enfoque quimiométrico para el estudio de cinodontes triásicos demostró ser útil para evaluar los cambios químicos de la microestructura ósea.

**Palabras clave.** Grupo Puesto Viejo. Fósildiagenesis. Mesozoico. Terápsidos no- mamaliformes. Quimiometría.

NON-MAMMALIAFORM therapsids dominated terrestrial ecosystems during the Late Paleozoic–Early Mesozoic. Among them, cynodonts have been studied in detail from a taxonomic, osteologic and functional morphology perspective (*e.g.*, Botha and Chinsamy, 2005; Ray *et al.*, 2004; Chinsamy and Abdala, 2008; Abdala and Ribeiro, 2010). However, their bone diagenesis has been poorly researched. This report is based on fossil remains of cynodonts found in southern Mendoza province,

Argentina. The fauna recorded in the Puesto Viejo Group is one of the oldest assemblages of Mesozoic tetrapods in South America. This fauna has a strong resemblance to African assemblages occurring in the *Cynognathus* Assemblage Zone of the Beaufort Group, South Africa (Kitching, 1995).

Scanning electron microscopy in combination with energy-dispersive X-ray spectrometry (SEM-EDX) is one of the most versatile and powerful analytical techniques for the de-

termination of major and minor inorganic components of different materials (*e.g.*, Goldstein *et al.*, 1992, 2007). The use of SEM-EDX has increased during the last decades mainly because of the non-destructive character and the relatively low-cost of analysis. Recently, SEM-EDX has proved useful in the study of the chemistry associated with different preservation modes in fossil remains (*e.g.*, Downing and Park, 1998; Kohn *et al.*, 1999; Rogers, *et al.*, 2001; Klug *et al.*, 2009; Lin and Briggs, 2010).

Cynodont remains from the Early Triassic of Mendoza, Argentina are studied for the first time using SEM-EDX. Semi-quantitative data derived from SEM-EDX spectra are evaluated by principal component analysis (PCA) to gain new insights regarding the likely chemical pathways affecting the bone microstructure.

## GEOLOGICAL SETTING

Lower Triassic non-marine sediments in Argentina are concentrated in the San Rafael Depocenter, located in southern Mendoza Province (Kokogian *et al.*, 2001). Extensional conditions in this basin allowed the deposition of the Puesto Viejo Group, which includes sedimentary, volcaniclastic and volcanic rocks, mostly light-gray and reddish in colour (Stipanicic *et al.*, 2007). This group was interpreted as (1) mid-distal alluvial fan deposits with coarse-grained lens and debris flows, (2) low- and high-sinuosity meandering fluvial systems with conglomeratic and sandstone lenses, crevasse channels and splays, and floodplains with local paleosols (Spalletti, 1994). The Puesto Viejo Group includes –from bottom to top– the

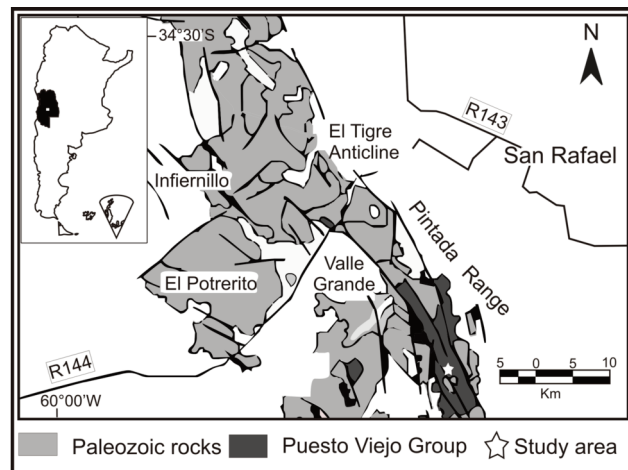


**Figure 1.** Location map of the Puesto Viejo Group showing the study area.

grayish Quebrada de los Fósiles Formation and the mostly reddish Río Seco de la Quebrada Formation (Stipanicic *et al.*, 2007). In the Quebrada del Durazno area (Fig. 1), the latter consists of lag-dominated channels, conglomeratic and sandstone bars (Gt, SGt, St, see in Spalletti, 1994) and floodplain facies (Fm, FTm, STm, Sm, see in Spalletti, 1994) with development of crevasse channel- and crevasse splay-deposits (St, Sl, Sh, see in Spalletti, 1994).

A cynodont rib (MHNSR-Pv 1160) was found in the floodplain facies characterized by red massive mudstone and fine-grained sandstone, locally with light greenish-grey mottled color and banded beds that suggest a high groundwater table. An appendicular bone of a cynodont (MHNSR-Pv 1162) was found in the crevasse splay facies characterized by red compact fine- to medium-grained sandstone highly bioturbated towards the top.

The material is deposited at the Museo de Historia Natural de San Rafael, Mendoza Province, Argentina (**MHNSR**).

## MATERIALS AND METHODS

The samples analyzed by means of petrographic and SEM-EDX techniques include a rib MHNSR-Pv 1160 (F1) and an appendicular bone MHNSR-Pv 1162 (F2) of the cynodonts mentioned above.

### Microscopic analysis

Thin sections of the fossil bones were prepared according to the techniques outlined by Chinsamy and Raath (1992) and were studied using a petrographic polarizing microscope (BX 51-P Olympus). Thin sections were used to analyze bone features such as mineral composition, fracturing and diagenetic deformation. Histological terminology and definitions follow Reid (1996) and Chinsamy-Turan (2005).

### EDX spectra

Elemental composition of the carbon-coated samples was obtained using a JEOL JSM-6610 LV scanning electron microscope equipped with an energy-dispersive spectrometer (Thermo Scientific Ultra Dry Noran System 7). Elements with atomic number greater than 5 were detected by the Sapphire Ultra-Thin Window X-ray detector, with a resolution of 129.2 eV for the Mn-K $\alpha$  line. An acquisition live time of 200 s, nominal incident beam energy  $E_0 = 15$  keV and 15 mm working distance were used in all cases. The inconsistency of take-

off angles between measured areas derived from the impossibility of using polished sample surfaces (see Goldstein *et al.*, 1992, 2007). Thus, the results provided by the standardless procedure are semi-quantitative. As a consequence, estimated statistical errors (not shown) in elemental concentrations can differ by as much as 15% of the values. The PROZA Phi-Rho-Z matrix correction algorithm (Bastin *et al.*, 1986) was used to perform matrix correction. Concentration data were transformed to 100 percent. This treatment admits no incompleteness and avoids the problem of biased correlation coefficients due to the closure effect (Zodrow, 1974).

Discriminating chemical patterns across bone-rock matrix transitions (BRT) proved useful to observe the redistribution of original hydroxyapatite  $[(\text{Ca}_{10}(\text{PO}_4)_6(\text{OH})_2)]$  or carbonate-bearing hydroxyapatite [dahllite,  $\text{Ca}_{10}(\text{PO}_4)_{6-x}(\text{CO}_3)_x(\text{OH})_{2+x}$ ] from bone and the likely incorporation of some elements into the bone microstructure. This was only performed in sample F1 (sample F2 is detached from the rock matrix).

Transect measurements were used to monitor trends in element distributions. Locations of measurement points were chosen at pre-set intervals. However, in some instances, point positions were manually modified to an adjacent area in order to avoid rock or bone pore spaces, thus ensuring a sufficiently flat surface area for the electron beam. Point-scans were performed from the bone through the bone-rock matrix interface towards the rock's edge. Distances between points were 0.25 mm. Weight percentage of major elements –O, F, Na, Mg, Al, Si, P, K and Ca, Mn and Fe–was determined at each point. They were selected in order to include major cations for rock-matrix minerals (*e.g.*, silicate, carbonate), commonly known enrichment constituents, major pore fillers (*e.g.*, Fe, Si) and species representing the original bone (*e.g.*, carbonate, phosphate).

#### ***Strategy for principal component analysis (PCA) of SEM-EDX data: a multivariate approach***

PCA, a nonparametric pattern-recognizing method, reduces the dimensionality of a data set consisting of a large number of variables, while retaining as much as possible the variance present in the original data set. This is achieved by transforming the original set of variables to a new set of variables, the principal components (PCs), which are linear combinations of the original variables. PCs are uncorrelated (orthogonal) and are ordered so that the first few encompass most

of the variation present in all the original variables (*e.g.*, Jolliffe, 2002; Lattin *et al.*, 2002; Rencher, 2002; Anderson, 2003; Johnson and Wichern, 2007; Izenman, 2008).

We retained the number of components of which the explained cumulative variance was close to 70% (Kaiser, 1960; see Kendall, 1965, for other methods). Other inherent assumptions included no error variance and underlying structure. Our strategy was to evolve a set of data groupings to evaluate it as a function of chemical composition derived from SEM-EDX spectra. PCA was performed using STATISTICA® (StatSoft Inc., 2004) on raw data consisting of 11 variables, with 27 determinations each.

PCA application is only a first approximation because of the uncertainty of the data. Advanced multivariate models (Zodrow, 1970; 1976), which presuppose that variables satisfy complex assumptions, cannot be used in this study.

## **RESULTS AND DISCUSSION**

This section includes the description of two samples collected from different environments, namely F1: rib, floodplain and F2: appendicular bone, crevasse splay.

#### ***Bone histology and mineral composition***

Calcium phosphate (*e.g.*, carbonate hydroxyapatite) constitutes the bones of vertebrate animals. During diagenesis some substitution of hydroxyl by fluorine may occur (Lucas and Prévôt, 1991). Therefore, hydroxyapatite –which is thermodynamically unstable– is usually transformed within the burial environment (Tuross *et al.*, 1989) by the incorporation of fluorine. SEM-EDX spectra indicate the presence of fluorine as shown by the peak at 0.67 keV (see section SEM-EDX), thus confirming recrystallization to francolite  $(\text{Ca}_{10}(\text{PO}_4)_5\text{CO}_3\text{F}_{1.5}(\text{OH})_{0.5})$ , which is a typical replacement of the fossilized bone (Elorza *et al.*, 1999; Rogers *et al.*, 2010).

**Rib (F1).** Analysis of thin sections shows a compact cortex surrounding a central cancellous region. The external cortex is formed by fibro-lamellar bone tissue with longitudinal primary osteons embedded in a woven bone matrix (Fig. 2.1–2). Toward the inner cortex, the perimedullary region shows extensive secondary reconstruction with abundant secondary osteons (Fig. 2.3–4). The medullary cavity contains endosteal trabeculae, especially in the proximal sections (Fig. 2.5–6).

The histological structure indicates that the main diagenetic processes affecting the bones were substitution of hy-

droxyapatite by francolite and permineralization (infiltration of mineral-bearing solutions into bony pores). The primary osteons and vascular channels are mainly filled by iron oxides and, to a lesser extent, calcite ( $\text{CaCO}_3$ ). Lithostatic

pressure and the consequent deformation of bone tissue caused complex fracture systems cutting across the vascular canals and thus modifying the original structure. Fossil-diagenetic processes include (1) a first event of hematite cementation on

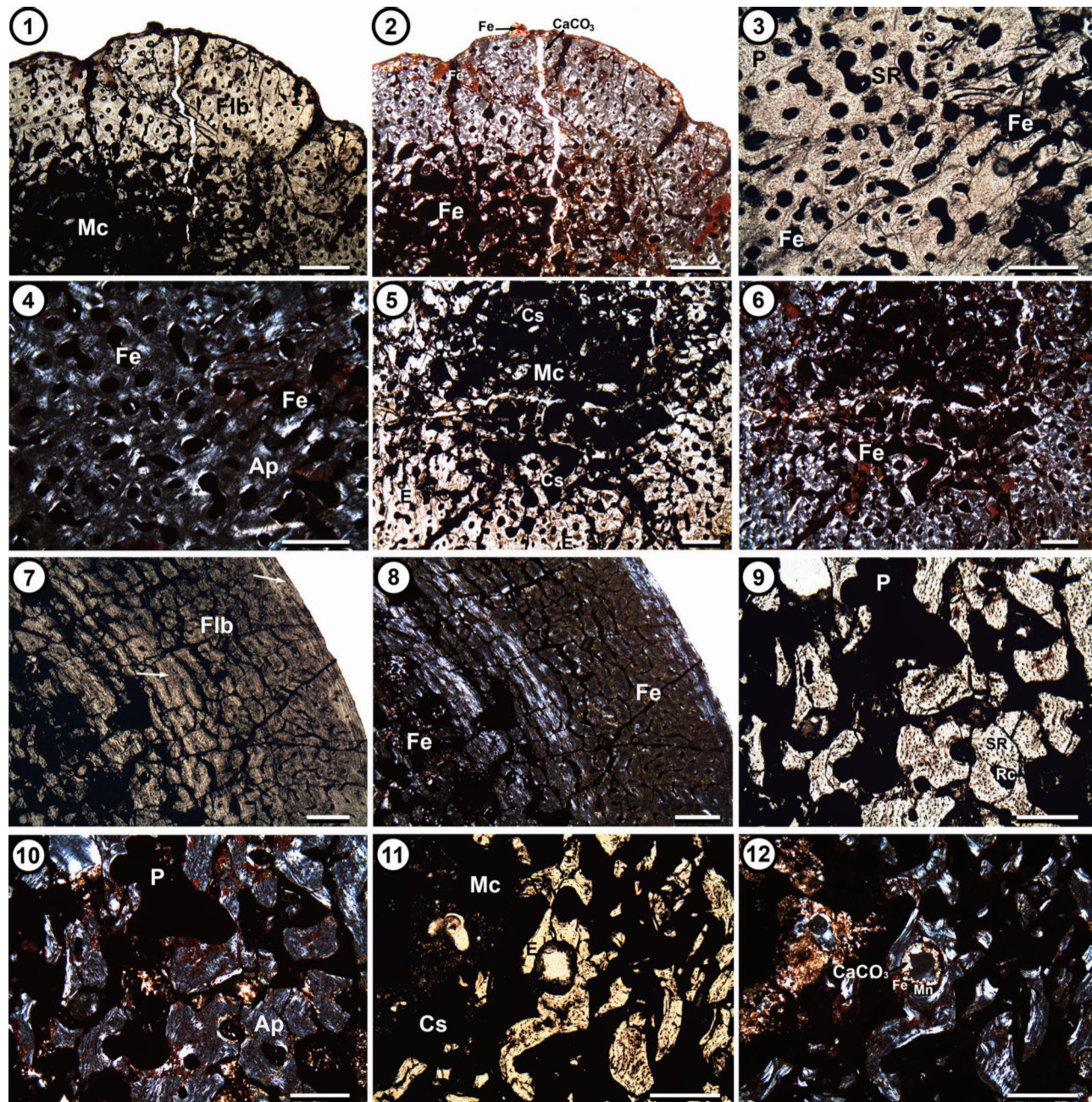


**Figure 2.** Transverse sections of cynodont bones. **1–6**, Rib, MHNSR-Pv 1160; **1**, cortical fibrolamellar bone with primary osteons and medullary cavity; **2**, external cortex with primary osteons and fractures infilled by hematite and calcite; **3–4**, perimedullary region showing secondary reconstruction with secondary osteons infilled by iron oxides; **5–6**, medullary cavity with endosteal trabeculae and cancellous spaces filled by hematite; **7–12**, appendicular bone, MHNSR-Pv 1162; **7**, fibrolamellar bone (subplexiform/laminar) with LAGs (arrows); **8**, oxide minerals coating on primary and secondary osteons, vascular canals and fractures; **9**, perimedullary region with resorption cavities and secondary reconstruction; **10**, fracturing and brittle deformation in secondary osteons and bony trabeculae; **11–12**, medullary cavity with cancellous spaces filled by iron minerals (Fe, Mn) and drusy calcite. Flb, fibrolamellar bone; P, perimedullary region; SR, secondary reconstruction; Rc, resorption cavity; Mc, medullary cavity; E, endosteal trabeculae; Cs, cancellous spaces; Ap, apatite; Fe, iron; Mn, manganese;  $\text{CaCO}_3$ , calcite. Photomicrographs (1, 3, 5, 7, 9, 11) in plane-polarized light; (2, 4, 6, 8, 10, 12) in cross polarized light. Scale bar = 1 mm.

vascular canals in medullary tissue and fractures (early diagenesis) (Fig. 2.2–6), (2) an event characterized by fracturing and brittle deformation due to lithostatic pressure (mesodiagenesis) (Fig. 2.2), (3) a stage of calcite precipitation in vascular canals and fractures (late diagenesis) (Fig. 2.2) and (4) a

stage including infiltration of iron carbonate minerals into the cortical wall (deep late diagenesis) (Fig. 2.2). The presence of calcite and iron enrichment (possibly corresponding to ferroan calcite) indicates local reducing conditions below the water-table during precipitation.

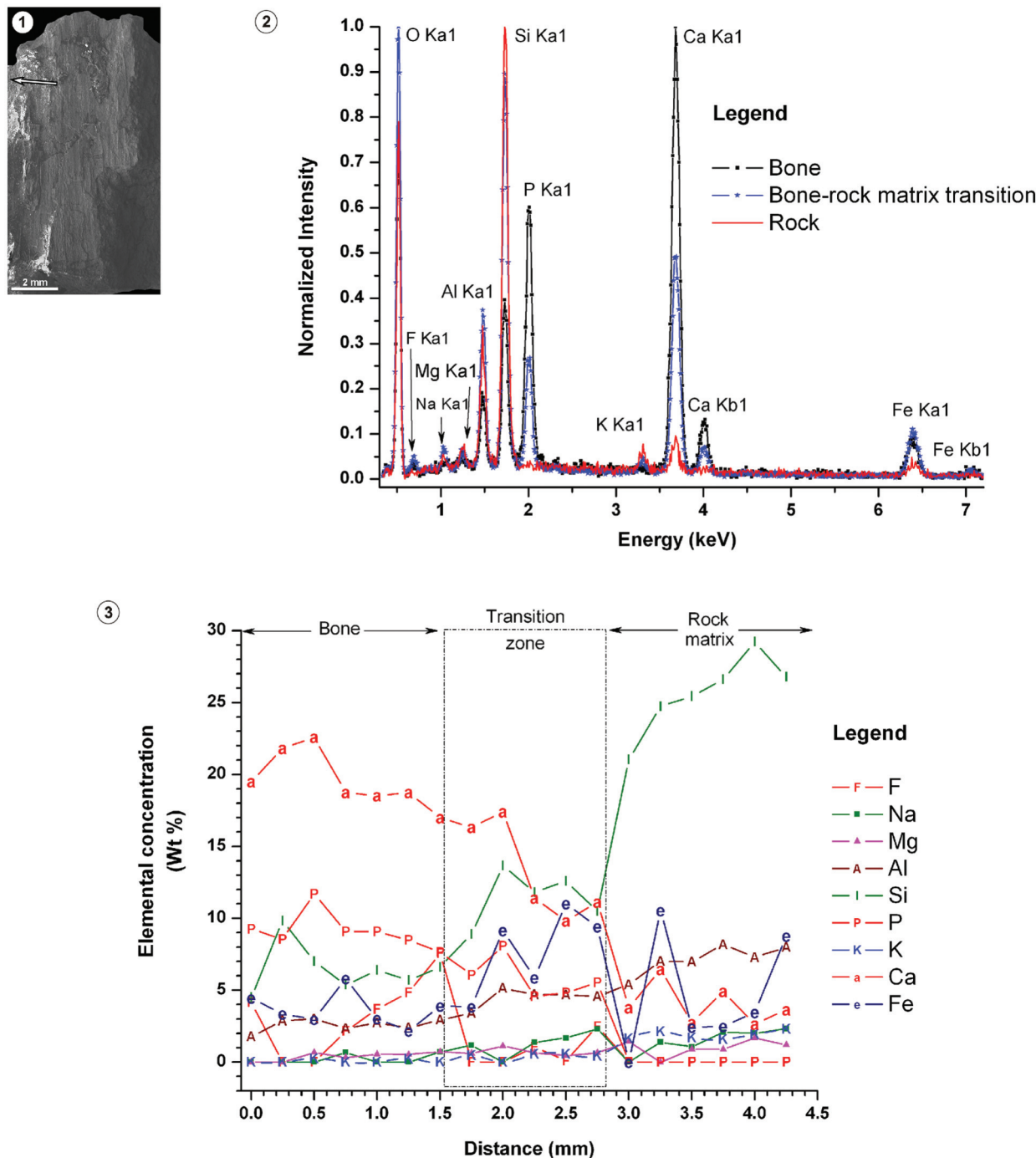


**Figure 3. 1–3,** SEM-EDX results. Sample: F 1; 1, Carbon-coated sample: SEM micrograph. Arrow indicates one of the approximate transect positions used for monitoring trends in elemental distributions by SEM-EDX; 2, X-ray spectra of representative sample zones; 3, Semi-quantitative results for point-scans across bone-rock matrix transition given as weight % (Wt %) versus distance. Scale bar= 2 mm (1).

**TABLE 1 - Semi-quantitative SEM-EDX results (elemental composition) given as weight % (Wt %)**

<b>Sample</b>	<b>Point Number*</b>	O	F	Na	Mg	Al	Si	P	K	Ca	Mn	Fe
Bone 1 (F1)												
	1	56.18	4.16	nd	nd	1.77	4.5	9.24	nd	19.48	nd	4.44
	2	53.57	nd	nd	nd	2.87	9.84	8.55	nd	21.82	nd	3.35
	3	51.18	nd	nd	0.68	3.01	7.02	11.7	0.25	22.59	nd	2.99
Bone	4	55.51	2.15	0.68	0.3	2.34	5.37	9.08	nd	18.74	nd	5.82
	5	55.89	3.67	nd	0.54	2.74	6.39	9.09	nd	18.51	nd	3.01
	6	56.94	4.85	nd	0.53	2.37	5.69	8.47	0.24	18.73	nd	2.18
	7	52.93	7.56	0.72	0.73	2.92	6.6	7.66	nd	16.99	nd	3.9
	8	59.23	nd	1.16	0.61	3.40	8.92	6.06	0.47	16.31	nd	3.84
Transition zone	9	45.46	nd	nd	1.11	5.14	13.66	8.08	nd	17.4	nd	9.16
	10	57.99	1.06	1.37	0.66	4.71	11.80	4.58	0.56	11.41	nd	5.86
	11	54.27	0.09	1.68	0.46	4.69	12.60	4.83	0.54	9.82	nd	11.02
	12	53.03	2.48	2.31	0.63	4.55	10.49	5.53	0.43	11.11	nd	9.42
	13	66.77	nd	nd	1.43	5.4	21.02	nd	1.62	3.77	nd	nd
	14	47.78	nd	1.39	nd	7.02	24.72	nd	2.13	6.45	nd	10.52
Rock matrix	15	58.4	nd	1.06	0.9	6.97	25.44	nd	1.68	2.75	nd	2.43
	16	53.22	nd	2.08	0.9	8.18	26.62	nd	1.59	4.93	nd	2.49
	17	51.77	nd	2.02	1.68	7.29	29.22	nd	1.94	2.63	nd	3.45
	18	47	nd	2.32	1.18	8.01	26.78	nd	2.3	3.65	nd	8.75
Bone 2 (F2)												
	na	42.78	nd	0.52	nd	0.72	2.4	13.78	nd	29.29	nd	10.52
	na	38.41	nd	0.57	0.15	0.66	2.07	15.52	0.67	34.52	nd	7.43
	na	30.07	nd	0.45	0.54	3.31	13.37	1.71	1.71	3.26	0.85	44.26
	na	40.18	nd	7.4	nd	11.49	31.61	1.01	0.42	2.2	1.66	4.04
	na	42.06	nd	0.95	nd	1	2.67	12.77	nd	27.53	nd	13.03
	na	46.97	nd	0.65	nd	0.5	1.52	15.57	nd	33.57	nd	1.21
	na	28.36	nd	1.06	nd	1.59	4.02	14.69	nd	42.13	nd	8.15
	na	37.58	nd	5.49	nd	7.49	19.88	1.43	0.72	2.84	1.14	23.44
	na	41.39	nd	4.52	0.29	6.36	18.84	1.84	1.28	4.32	1.96	19.22

\* point-scans across bone-rock matrix transition. na: not applicable. nd: not detectable

**Appendicular bone (F2).** The bone diaphysis section shows a thick cortex surrounding a medullary cavity. The fibrolamellar bone shows primary osteons arranged in a sub-plexiform to laminar pattern (Fig. 2.7–8). Lines of arrested growth (LAGs) are present in the outer and mid-cortical region (arrows in Fig. 2.7). Erosionally enlarged resorption cavities and secondary osteons are visible in the perimedullary region, (Fig. 2.9–10). Internal to this region is a zone of compacted coarse cancellous bone. The medullary cavity contains large cancellous spaces and endosteal bony trabeculae (Fig. 2.11–12).

Sample F2 shows similar diagenetic processes to those in F1. However, the substitution of hydroxyapatite by francolite was not recorded. Both areas (cortical and medullary) show vascular canals and endosteal trabeculae mainly filled by iron and manganese minerals (*e.g.*, hematite, manganite) and calcite. The perimedullary region and bony trabeculae show fracturing and brittle deformation (collapse of the spongy tissue)

due to lithostatic pressure (Fig. 2.9–12). Fossil-diagenetic processes observed herein include (1) an initial oxide minerals coating on primary and secondary osteons, vascular canals and fractures (early diagenesis) (Fig. 2.8), (2) fracturing and brittle deformation in trabeculae and pore spaces (mesodiagenesis) (Fig. 2.10–12), (3) a third event of drusy calcite cementation in vascular canals and cancellous spaces (late diagenesis) (Fig. 2.12) and (4) final infiltration of iron imposed onto the medullary tissue (Fig. 2.12). This may be a result of late diagenetic oxidization of iron minerals.

Fossil-diagenetic processes observed in this study include substitution, fracturing, brittle deformation and hematite, manganite and calcite permineralization events. Similar diagenetic features have been identified in dinosaur bones from Cretaceous floodplain deposits in the Neuquén Basin in Mendoza (González Riga and Astini, 2007; González Riga *et al.*, 2009).

### SEM-EDX

Figure 3.1 shows a representative SEM micrograph of the carbon-coated sample (F1). The arrow indicates the approximate position of one of the transects used for monitoring trends in SEM-EDX elemental distributions. The X-ray spectra of representative sample zones are illustrated in Fig. 3.2. Sample F2 (detached from the rock matrix as noted above) exhibits similar X-ray spectra (not shown). Transect measurements taken across BRT yielded distribution patterns of major and minor elements as depicted in Figure 3.3. Bone constituents (P and Ca) are correlated throughout the bone and into the rock matrix. At the BRT, Ca and P concentrations drop off for a small distance (approximately 0.8 mm in the figured example). This is particularly evident in Ca concentrations varying from a maximum of 22.6% in the bone structure to a minimum value of 2.63% in the rock matrix.

High Fe concentrations mark the bone/rock boundary (approximately 10%, Fig. 3.3) and presumably represent ferroan calcite, which is visible microscopically on the inner bone surface (Fig. 2.2). Si and Fe are concentrated mainly in the rock matrix (Fig. 3.2–3), though Fe may fill bone voids. The other elements examined, *i.e.*, Na, Mg, Al, K (Fig. 3.3) and O (not plotted) show minor differences in concentration around the BRT.

Higher F concentrations (up to 7.56%; Fig. 2.3) within the bone microstructure are considered supportive evidence of the diagenetic replacement of this element.

In the following section, a more comprehensive evaluation of the complete set of semi-quantitative SEM-EDX data (samples F1 and F2; Tab. 1) is performed by means of PCA.

### Principal component analysis (PCA)

The larger number of data points (297: 27 cases and 11 attributes; Tab. 1) provides an opportunity for PCA to focus on grouping data as a function of chemical composition (see Appendix in Supplementary Online Material).

Cumulatively, two components account for 72.1% of the variance; the loading plots and scores are shown in Figure 4.1 and 4.2, respectively. The most important component (47.89% of the explained variance) involves positive and negative loadings, highlighting the presence of P, Ca and F (apatite) *vs.* the other elements (*i.e.*, Mg, Na, Si, K and Al) (silicates). Points measured on the bone structure (F1 and F2) exhibit the most negative scores (Fig. 4.2; x axis), reflecting

their high contents of P and Ca, as well as moderate F contents in F1 (fluorine was not detectable in F2). Scores against the first principal component clearly indicate the differences amongst the three areas (*i.e.*, bone, transition zone and rock matrix) in F1. The group representing the transition zone in F1 is separated from the other groups (Fig. 4), indicating an intermediate composition between bone and rock matrix.

F2 scores against the first component indicate two groupings representing clearly different compositions. One of them (Fig. 4.2; lower right quadrant) indicates a composition more similar to the rock matrix than to the bone. In this case measurements were performed on selected points of the medullary cavity containing endosteal trabeculae filled by Mn and Fe minerals (*e.g.*, manganite, hematite).

The second component (24.21% of accounted variance) involved positive loadings on O and Mg, and negative loadings on Fe and Mn. The points measured on the bone structure (F1) show positive scores against this component (Fig. 4.2; y axis), as a result of the relatively low Fe concentrations being amongst the lowest in the entire sample set (Tab. 1). Con-

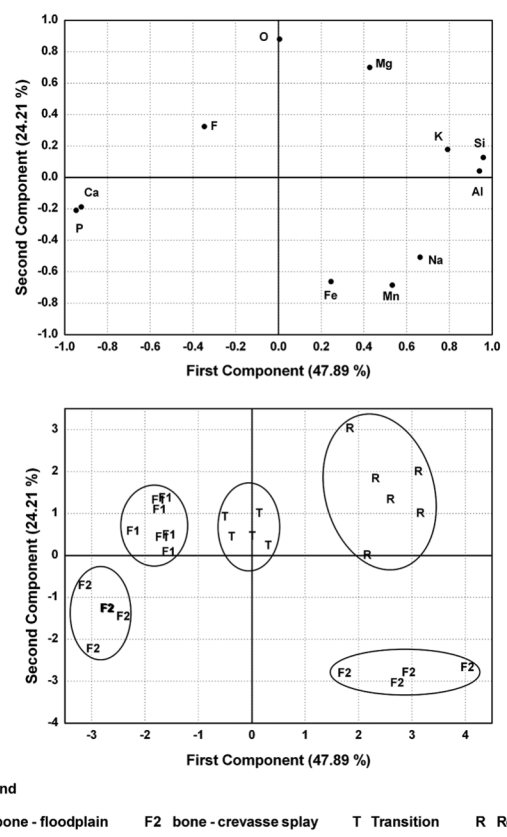


**Figure 4. 1–2.** PCA plots; 1, component loadings; 2, component scores. See text for explanation of PCA. Approximately elliptical delimited zones are used for clarity only and bear no statistical significance.

versely, points measured on F2 exhibit negative scores against the second component mainly because of the high Fe concentrations and the presence of Mn. This is likely related to the facies –crevasse splay– where F2 was found.

The plot of scores was particularly useful in showing the different grouping of data as a function of chemical composition and in reflecting the nature of the different sample areas analyzed. Results suggest a relationship between bone groupings and different facies (floodplain and crevasse splay), though the number of samples studied is still limited. Ellipses around the groupings (Fig. 4.2) are for clarity only and have no statistical significance.

## CONCLUSIONS

This spectrometric study (SEM-EDX) allows the following conclusions:

1. The multivariate model supports the distinction of different specimen areas in terms of chemical parameters (major and minor chemical elements), *i.e.*, bone, transition zone and rock matrix. Differentiation is based mainly –but not exclusively– on varying contents of Ca, P, F, Si, Al and K, as well as of O, Mn and Fe. It is also suggested that variable concentrations of Fe and Mn could be related to features of the different facies (*i.e.*, floodplain and crevasse splay).

2. These results along with thin section petrographical analysis confirm, in one of the cases, the substitution of hydroxyapatite by fluorapatite into the bone microstructure.

The content of F (fluorine) in F1 (not detectable in F2) confirmed differences between the two samples and their depositional environments. The original apatite framework is mainly filled by iron minerals and carbonates brought about by different diagenetic events. Fossil-diagenetic processes observed herein include substitution, fracturing, brittle deformation, and different permineralization events. Permineralization stages include infilling of vascular canals, trabeculae and fractures with hematite, manganite and calcite during burial history.

3. This chemometric methodology for the diagenetic study of the Triassic cynodont bones is an efficient approach to elucidate the likely chemical pathways affecting bone microstructure.

## ACKNOWLEDGEMENTS

We thank M. de la Fuente (Museo de Historia Natural de San Rafael, Mendoza) for facilitating the studied material. The IANIGLA-CCT-Mendoza

provided assistance during laboratory works (electron and petrographic microscopes). Our thanks are due also to the journal reviewers, E.L. Zodrow (Cape Breton University, Canada), and an anonymous reviewer. They suggested significant changes which improved the quality of presentation of the manuscript. We thank T. Heredia for the critical reading of the manuscript. This research is supported by projects PICT BID 07-373 (M. de la Fuente), PIP CONICET 2009/10 (A.C. Mancuso) and Universidad Nacional de Cuyo (ICB, SeCTyP Research Project 06/M038).

## REFERENCES

- Abdala, F., Ribeiro, A.M., 2010. Distribution and diversity patterns of Triassic cynodonts (Therapsida, Cynodontia) in Gondwana. *Palaeogeography, Palaeoclimatology, Palaeoecology* 286: 202–217.
- Anderson, T.W. 2003. *An Introduction to Multivariate Statistical Analysis; Wiley Series in Probability and Statistics, third edition*. John Wiley & Sons, Hoboken, 752 p.
- Bastin, G.F., Van Loo, F.J.J. and Heijliger, H.J.M. 1986. Evaluation of the use of Gaussian  $\phi$  ( $\rho_z$ ) curves in quantitative electron probe microanalysis: A new optimization. *X-Ray Spectrometry* 13: 91–97.
- Botha, J., Chinsamy, A. 2005. Growth patterns of *Thrinaxodon liorhinus*, a non-mammalian cynodont from the Lower Triassic of South Africa. *Palaeontology* 48: 385–394.
- Chinsamy-Turan, A. 2005. *The microstructure of dinosaur bone*. The Johns Hopkins University Press, Baltimore and London, p. 1–194.
- Chinsamy, A. and Abdala, F. 2008. Palaeobiological implications of the bone microstructure of South American traversodontids (Therapsida: Cynodontia). *South African Journal of Science* 104: 225–230.
- Chinsamy, A. and Raath, M.A. 1992. Preparation of fossil bone for histological examination. *Palaeontologia Africana* 29: 39–44.
- Downing, K.F. and Park, L.E. 1998. Geochemistry and Early Diagenesis of Mammal-Bearing Concretions from the Sucker Creek Formation (Miocene) of Southeastern Oregon. *Palaios* 13: 14–27.
- Elorza, J., Astibia, H., Murelaga, X. and Pereda-Suberbiola, X. 1999. Franclite as a diagenetic mineral in dinosaur and other Upper Cretaceous reptile bones (La Rioja, Iberian Peninsula): microstructural, petrological and geochemical features. *Cretaceous Research* 20: 169–187.
- Goldstein, J.I., Newbury, D.E., Echlin, P., Joy, D.C., Romig, A.D., Jr., Lyman, C.E., Fiori, C. and Lifshin, E. 1992. *Scanning Electron Microscopy and X-ray Microanalysis: A Text for Biologists, Material Scientists and Geologists; second Edition*. Plenum Press, New York, 820 p.
- Goldstein, J.I., Newbury, D.E., Joy, D.C., Lyman, C.E., Echlin, P., Lifshin, E., Sawyer, L.C. and Michael, J.R. 2007. *Scanning Electron Microscopy and X-ray Microanalysis; third edition*. Springer, New York, 586 p.
- González Riga, B.J. y Astini, R. 2007. Preservation of large titanosaur sauropods in overbank fluvial facies: A case study in the Cretaceous of Argentina. *Journal of South American Earth Sciences* 23: 290–303.
- González Riga, B.J., Previtera, E. y Pirrone, C.A. 2009. *Malarguesaurus florenciae* gen. et sp. nov., a new titanosauriform (Dinosauria, Sauropoda) from the Upper Cretaceous of Mendoza, Argentina. *Cretaceous Research* 30: 135–148.
- Izenman, A.J. 2008. *Modern Multivariate Statistical Techniques: Regression, Classification and Manifold Learning. Springer Texts in Statistics; first edition*. Springer, New York, 734 p.
- Johnson, R.A., Wichern, D.W. 2007. *Applied Multivariate Statistical Analysis; sixth edition*. Prentice Hall, Upper Saddle River, 800 p.
- Jolliffe, I.T. 2002. *Principal Component Analysis; second edition*. Springer, New York, 487 p.
- Kaiser, H.F. 1960. The application of electronic computers to factor analysis. *Educational and Psychological Measurement* 20: 141–151.
- Kendall, M.G. 1965. *A Course in Multivariate Analysis; third Impression*. Charles Griffin & C. Ltd., London. 185 p.

- Kitching, J.W. 1995. Biostratigraphy of the *Cynognathus Assemblages Zone*. *South African Committee for Stratigraphy and Biostratigraphy Series* 1: 40–45.
- Klug, C., Schulz, H. and De Baets, K. 2009. Red Devonian trilobites with green eyes from Morocco and the silicification of the trilobite exoskeleton. *Acta Palaeontologica Polonica* 54: 117–123.
- Kohn, M.J., Schoeninger, M.J., Barker, W.W. 1999. Altered states: Effects of diagenesis on fossil tooth chemistry. *Geochimica et Cosmochimica Acta* 63: 2737–2747.
- Kokogian, D.A., Spalletti, L.A., Morel, E.M., Artabe, A.E., Martínez, R.N., Alcober, O.A., Milana, J.P., Zavattieri, A.M. 2001. Estratigrafía del Triásico argentino. In: A.E. Artabe, E.M. Morel, A.B. Zamuner,(Eds.), *El Sistema Triásico en la Argentina*. Fundación Museo de la Plata “Francisco Pascasio Moreno”, La Plata, p. 23–54.
- Lattin, J., Carroll, D., Green, P. 2002. *Analyzing Multivariate Data (Duxbury Applied Series); first edition*. Duxbury Press, Belmont, 560 pp.
- Lin, J.P., Briggs, D.E.G. 2010. Burgess shale-type preservation: a comparison of naraoiids (Arthropoda) from three Cambrian localities. *Palaios* 25: 463–467.
- Lucas, J. and Prévôt, L.E. 1991. Phosphates and Fossil Preservation. In: P.A. Allison and D.E.G. Briggs (Eds.), *Taphonomy: Releasing the Data Locked in the Fossil Record; Topics in Geobiology, volume 9*. Plenum Press, New York, p. 389–409.
- Ray, S., Botha, J. and Chinsamy A. 2004. Bone histology and growth patterns of some nonmammalian therapsids. *Journal of Vertebrate Paleontology* 24: 634–648.
- Reid, R.E.H. 1996. Bone histology of the Cleveland-Lloyd dinosaurs and of the dinosaurs in general, Part I: Introduction: Introduction to bone tissues. *Geology Studies* 41: 25–71.
- Rencher, A.C. 2002. *Methods of Multivariate Analysis, Volume 1; Wiley Series in Probability and Statistics Series, second edition*. John Wiley & Sons, Hoboken, 738 p.
- Rogers, R.R., Arcucci, A.B., Abdala, F., Sereno, P.C., Forster, C.A., May, C.L., 2001. Paleoenvironment and Taphonomy of the Chañares Formation Tetrapod Assemblage (Middle Triassic), Northwestern Argentina: Spectacular Preservation in Volcanogenic Concretions. *Palaios* 16: 461–481.
- Rogers, R.R., Fricke, H.C., Addona, V., Canavan, R.R., Dwyer, C.N., Harwood, C.L., Koenig, A.E., Murray, R., Thole, J.T. and Williams, J. 2010. Using laser ablation-inductively coupled plasma-mass spectrometry (LA-ICP-MS) to explore geochemical taphonomy of vertebrate fossils in the Upper Cretaceous Two Medicine and Judith River formations of Montana. *Palaios* 25: 183–195.
- Spallarti, L.A. 1994. Evolución de los ambientes fluviales en el Triásico de la Sierra Pintada (Mendoza, Argentina): análisis sobre la influencia de controles intrínsecos y extrínsecos al sistema deposicional. *Revista de la Asociación Argentina de Sedimentología* 1: 125–142.
- StatSoft, Inc. 2004. *STATISTICA* (Data Analysis Software System), Version 7. <[www.statsoft.com](http://www.statsoft.com)>.
- Stipanicic, P.N., González Díaz, E.F., Zavattieri, A.M. 2007. Grupo Puesto Viejo nom. transl. por Formación Puesto Viejo González Díaz, 1964, 1967: nuevas interpretaciones paleontológicas, estratigráficas y cronológicas. *Ameghiniana* 44: 759–761.
- Tuross, N., Behrensmeyer, A.K., Eanes, E.D., Fisher, L.W. and Hare, P.E. 1989. Molecular preservation and crystallographic alterations in a weathering sequence of wildebeest bones. *Applied Geochemistry* 4: 261–270.
- Zodrow, E.L. 1970. Factor analyses and magnetite formation and distribution in the Smallwood Mine. *Society of Mining Engineers, AIME, Transactions* 247: 61–69.
- Zodrow, E.L. 1974. Note on closure correlation. *Canadian Journal of Earth Sciences* 11: 1616–1619.
- Zodrow, E.L. 1976. Minres factor analysis of hypersthene data, Strathcona Mine (Ontario, Canada). *Mathematical Geology* 8: 395–412.

doi: 10.5710/AMGH.2.7.2013.623

**Recibido:** 29 de octubre de 2012**Aceptado:** 2 de julio de 2013